DOI: 10.31276/VJSTE.64(2).03-09

Investigation of the water states of poly(styrene sulfonic acid) grafted poly(ethylene-co-tetrafluoroethylene) copolymer using FT-IR analysis

Tran Trong Hieu Dinh[1], Hoang Hao Lam[2], Thanh Danh Tran[2], Quang Luan Le[3], Van Man Tran[2], Truc Phuong Huynh[2], Van Phuc Dinh[4], Anh Tuyen Luu[5], Kim Ngoc Pham[2], Duy Tap Tran[2*]

[1]Physics Laboratory, Le Thanh Ton High School, Ho Chi Minh city
[2]University of Science, Vietnam National University, Ho Chi Minh city
[3]Biotechnology Center of Ho Chi Minh city
[4]Institute of Fundamental and Applied Sciences, Duy Tan University, Ho Chi Minh city
[5]Center for Nuclear Technologies, Vietnam Atomic Energy Institute, Ho Chi Minh city

Received 19 April 2021; accepted 24 June 2021

Abstract:

The water states of poly(styrene sulfonic acid) (PSSA) grafted poly(ethylene-co-tetrafluoroethylene) copolymers (ETFE-PEMs) with grafting degree (GD)=8.8-30.5% are investigated under ambient conditions by using FT-IR analysis. Detailed analysis of the FT-IR spectra of ETFE-PEMs allows the observation of each component of water in the two broad bands of 1500-2000 cm^{-1} and 2400-3800 cm^{-1}. These components include protonated water (H_3O^+…$(H_2O)_n$), H-bonded water to sulfonic acid groups ((SO_3)…$(H_3O^+)(H_2O)_n$), H-bonded water to other water molecules ((H_2O)…(H_2O)), and non-H-bonded water (HOH…F). Of these water forms, ((SO_3)…$(H_3O^+)(H_2O)_n$) is predominantly represented. Free water (non-H-bonded water) is assumed to be trapped in the holes of the ETFE backbone and is thus difficult to remove at 50°C over a 24 h period. The total peak areas of the water molecules significantly increase with GD indicating that the ETFE-PEM with higher GD possesses higher water content. Moreover, the increase of the total peak area with GD via two steps reveals an interesting relationship between the hierarchical structures and the capacity of water content under ambient conditions. The observed water content at ambient conditions can significantly affect the conductance of ETFE-PEMs under conditions of low relative humidity such as during fuel cell operation or measurement procedures of specific characterisations or testing methods.

Keywords: **ETFE, FT-IR, pre-irradiation grafting, water states.**

Classification number: **2.1**

Introduction

A hydrogen fuel cell is an electrochemical device that converts energy from the chemical reaction of hydrogen fuel into electrical energy (electricity). This device exhibits several advantages such as high efficiency (60% or higher), low temperature operation (~100°C), and zero waste emission as the by-products are only heat, water, or steam when only hydrogen and air are the reactants [1]. Fuel cells are thriving in the automobile industry as this fuel source is being developed by the world's leading automobile companies such as General Motors (USA), Ford (USA), Daimler Benz (Germany), Renault (France), Toyota (Japan), Nissan (Japan), Honda (Japan), and Hyundai (Korea). Indeed, the potential of these fuel cells in life-service industries is enormous [2]. In addition to transportation, power generation, and heat applications, fuel cells are also utilised in mobile applications like mobile phones and laptops [3]. Proton exchange membranes or polymer electrolyte membranes (PEMs) are the core and most critical component of a proton exchange membrane fuel cell (PEMFC) because it acts to conduct protons from the anode to the cathode, prevents hydrogen and oxygen diffusion across the membrane, and thus is involved in energy efficiency and durability of fuel cells [4]. Currently, the most popular material used to make PEM is Nafion, but this material faces some limitations such as low proton conductivity with increasing temperature (>70°C) and decreasing relative humidity (RH) (RH <50%), high gas permeation, and high cost [5]. This has prompted scientists to find new materials to replace Nafion.

*Corresponding author: Email: tdtap@hcmus.edu.vn

Among the many new candidate materials, PSSA grafted ETFE-PEMs exhibit several advantages such as high proton conductivity, good heat resistance, good chemical stability, moderate water absorption, and high mechanical stability [6]. Thus, this graft-type PEM has been extensively investigated by our group and others [7-11]. During characterisation of PEMs for hydrogen fuel cell applications, many measurement procedures and testing methods have been realised to study the water content or water state in PEMs including ion exchange capacity (IEC), water uptake, mechanical strength, proton conductivity, thermogravimetric analysis (TGA), differential scanning calorimetry (DSC), positron annihilation spectroscopy, X-ray photoelectron spectra (XPS), etc. [12]. The amount of water absorbed in the surrounding environment can affect the subsequent water absorption when PEM is placed in an environment with higher RH or total hydration [9] and thus it is involved in the conductance of membranes under conditions of low RH [13, 14]. However, there have been no reports about this critical issue despite its importance in obtaining precise results from the abovementioned characterization methods and as the primary step toward understanding the water absorption and proton conductance mechanisms under various RH conditions and especially at very low RH.

Therefore, in this study, we report an examination of the water states of ETFE-PEMs with GD=8.8-30.5% by using FT-IR spectroscopy as this technique is very sensitive to the existence of water molecules even at a very small amount [14]. The states of water are investigated and discussed by using FT-IR analysis as a function of GD. This study provides the first insights into water states in graft-type PEMs in their ambient environment.

Materials and methods

Materials

ETFE films of 50-µm thickness were provided by Asahi Glass Co. Ltd., Japan. Styrene, sodium chloride, 1,2-dichloroethane, and sodium hydroxide were provided by Wako Pure Chemical Industries, Ltd., Japan. Acetone, sulfonic acid, toluene, and hydrogen peroxide were purchased from Wako Pure Chemical Industries, Ltd. All the organic chemicals were used without further purification [7, 8].

Preparation

The general procedures for preparation and an illustration of the chemical structures of ETFE and ETFE-PEM are depicted in Scheme 1. All materials, reagents, and details on the preparation of ETFE-PEMs using the pre-irradiation grafting method have been previously described [7, 8]. Briefly, the ETFE films were irradiated by gamma rays emitted from a ^{60}Co source (Japan Atomic Energy Agency in Takasaki, Japan) under argon conditions with an absorbed dose of 15 kGy and a dose rate of 15 kGy/h. The irradiated samples were then immersed in a styrene solution (in toluene solvent) with different concentrations at 60°C for graft polymerization to obtain polystyrene-grafted ETFE films. The GD is determined based on the formula: GD (%) = 100*(W_g - W_0)/W_0, where W_0 and W_g are the weights of pristine ETFE and the grafted film, respectively. The grafted films were soaked in a 0.2-M chlorosulfonic acid solution in a 1,2 dichloroethane solvent at 50°C for about 6 h of sulfonation to obtain ETFE-PEMs [8, 9].

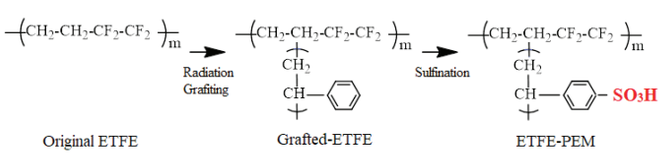

Scheme 1. Synthetic scheme and molecular structures for ETFE-PEMs using pre-irradiation grafting of styrene onto the ETFE substrate and subsequent sulfonation [9].

FT-IR measurement

The chemical structures and water states of the pristine ETFE and ETFE-PEMs were investigated by using Fourier-transform infrared (FT-IR) spectroscopy in absorption mode at the Center for Nuclear Technologies in Ho Chi Minh city, Vietnam. Before the FT-IR measurements, the ETFE-PEMs were dried in a vacuum oven at 50°C for 24 h to remove the remaining water molecules inside the membranes. FT-IR spectra were recorded using a spectrometer (IRAffinity1, Shimadzu, Japan) at wavenumbers ranging from 400 to 7000 cm^{-1} over the course of 64 scans with a resolution of 4 cm^{-1} at room temperature.

Results and discussion

FT-IR spectra of the original ETFE and the ETFE-PEMs with GD ranging between 8.8-30.5% are shown in Fig. 1. The FT-IR spectrum of pristine ETFE was reported previously [10]. Briefly, the film is characterised by strong bands in the wavenumber range of 1000-1400 cm^{-1}, which identifies the CF_2 groups. In addition, the CH_2

asymmetric stretching vibration rises around 2974 and 2879 cm^{-1} and the sharp band at 1452 cm^{-1} is assigned to the -CH deformation [11]. After grafting and sulfonation, all the ETFE-PEMs show the similar characteristic peaks of original ETFE plus new peaks at 1492 and 1600 cm^{-1} that are ascribed to deformation of the conjugated C=C of the benzene ring. In addition, bands appeared at 756 and 698 cm^{-1}, which are assigned to CH out-of-plane vibration, and the bands found at 3020-3010 cm^{-1} are ascribed to C-H stretching [15]. These spectral features indicate that styrene was indeed grafted onto the ETFE film. Also observed are absorption bands at 840 and 607 cm^{-1} due to the stretching vibration of S=O and the two broader bands of 1500-2000 cm^{-1} and 2400-3800 cm^{-1} are due to the existence of water molecules. These peak features indicate that the grafted film was sulfonated by the introduction of the $-SO_3H$ group [15]. Also seen in Fig. 1 is the significant increase in the broad bands of 1500-2000 cm^{-1} and 2400-3800 cm^{-1} with the increase of GD, which indicates that ETFE-PEM with higher GD possesses more water content despite ambient conditions. Surprisingly, the source of the water content has not been clear until now. Indeed, the source may originate from the fact that the membranes re-absorbed water after treatment at 50°C for 24 h as described in the Experimental section and/or free waters, which are confined in the free-volume holes of the crystallite phases and/or bonded waters, which are assigned to the strong hydrogen bonding effect between sulfonic acid groups and water [11].

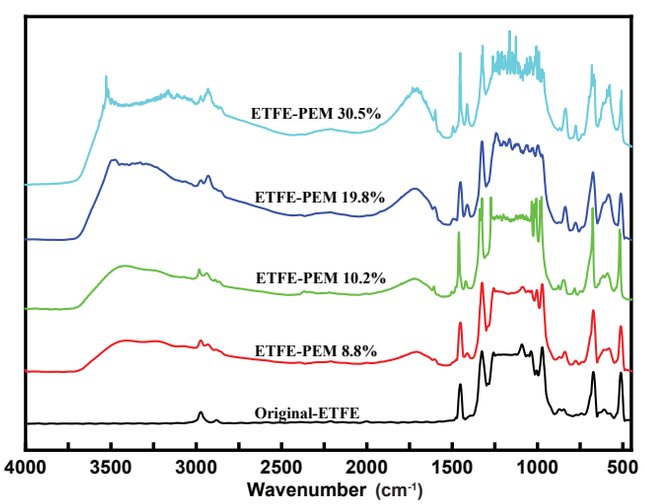

Fig. 1. FT-IR spectra of the original ETFE film and ETFE-PEMs with GD ranging between 8.8 and 30.5%.

There have been reports that water content dramatically affects several measurements of the graft-type PEMs such as XPS [15], IEC [15, 16], PALS [15], or the conductance of membranes at low RH [13]. Thus, in the following sections, we performed the analysis of FT-IR spectra in detail to explore the water states and water content in ETFE-PEMs with various GD values.

Figure 2 shows the FT-IR spectrum of ETFE-PEM (GD=10.2%) with a band at 1500-2000 cm^{-1} due to the bent oscillation of the -OH group plus a peak at 1600 cm^{-1} representing the C=C group of polystyrene grafted onto the pristine film as represented above. Thus, the spectrum is deconvoluted into four component peaks including peak1 at 1636 cm^{-1} (assigned to the -OH group's bending oscillation in $(H_2O)_n$), peak2 at 1700 cm^{-1} (attributed to the bending oscillation of the -OH group in hydronium (H_3O^+)), peak3 at 1788 cm^{-1} (representing the bending oscillation of -OH group in large protonate groups such as the ions Zundel ($H_5O_2^+$) and Eigen ($H_9O_4^+$)) [17], plus the peak at 1600 cm^{-1} of C=C. The above assignments are based on the fact that the O-H bond length in $(H_2O)_n$ is the smallest, followed by H_3O^+, and then the large protonate group. A considerable bond length leads to a small bonding force and, thus, the bending energy is enormous, which is why the large protonate group is located at the largest wavenumber [18].

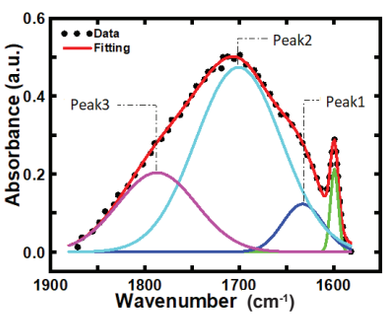

Fig. 2. A deconvolution model for FT-IR spectrum of ETFE-PEM with GD=10.2% in the spectral region of 1500-2000 cm^{-1}.

The oscillation frequency of the peaks represents the bent oscillation of the OH group so that the changes in the position of the peaks and peak intensity can be compared. Fig. 3A shows the spectrum of each component peak, and the results indicate that the peak positions of all membranes do not change with GD. However, contrary to the peak positions, the peak areas (Fig. 3B) change significantly with GD and follows the order of peak2 (H_3O^+) > peak3 ($H_5O_2^+$) > peak1 $(H_2O)_n$. Moreover, H_3O^+ is predominantly represented, which indicates that the hydrogen bonds connecting protonate and H_2O are preferred in all the ETFE-PEMs. The result can be explained by the fact that the PSSA groups can reach and elongate in free water clusters. These

free water clusters continue to participate in the group dissociation process, i.e., $-SO_3H + H_2O \rightarrow -SO_3^- + H_3O^+$ and the combines with free water $(H_2O)_n$ to create H_3O^+, $H_5O_2^+$, or larger clusters. Therefore, the content of free water $(H_2O)_n$ is small while the water component of H_3O^+, $H_5O_2^+$, and $H_9O_4^+$ increases with GD [19]. This result leads to an assumption that, under ambient conditions, the ETFE-PEMs possess water molecules that are mainly located around the PSSA groups but these amounts of water are not large enough to form water channels.

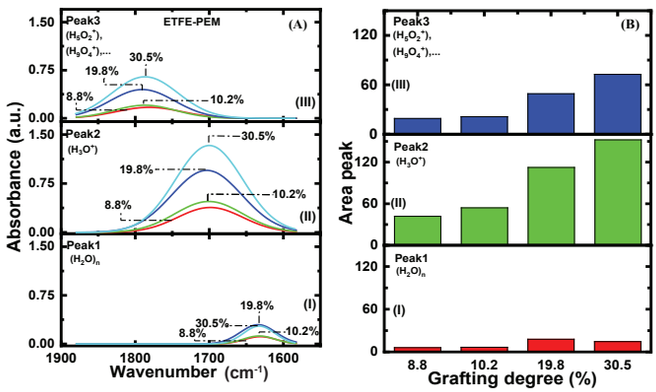

Fig. 3. FT-IR spectra of ETFE-PEMs with GD=8.8-30.5% in the band region of 1500-2000 cm^{-1} for (A) each component peak and (B) the corresponding peak area.

Figure 4 shows the FT-IR spectrum in the band region of 2400-3800 cm^{-1} of ETFE-PEM with GD=10.2%. This band represents the drag oscillation of the -OH group. In this region, water modes are classified into hydrogen-free water containing "mixture" waters located in the larger band region and a "continuum" of water possessing the hydrogen bonds that form a network located at the smaller band region [17]. Thus, the spectrum is deconvoluted into nine component peaks including five peaks relating to water molecules and four peaks representing PS grafts and pristine ETFE. Peak1 at 2669 cm^{-1} is assigned to the symmetric tensile oscillation of HO…H in the protonated water species hydronium (H_3O^+) [17, 20]. Peak2 at 3032 cm^{-1} is attributed to the tensile oscillation of the O-H bond in the protonate group that directly interacts with the $-SO_3^-$ group according to the model $(SO_3^-)…(H_3O^+)(H_2O)_n$ [21]. Peak3 at 3260 cm^{-1} is assigned to protonated water species in the form of a Zundel cation $(H_5O_2^+)$ [21]. Peak4 at 3441 cm^{-1} is attributed to O-H stretching vibrations of H-bonded water molecules to other water molecules $[(H_2O)…(H_2O)]$ and is also referred to as "bulk water" [21]. Because of the existence of the extracellular hydrogen spherical bonds HO…H in the form of a Zundel cation $(H_5O_2^+)$, peak3 is located at a position where the wavenumber is greater than peak1 and peak2 but smaller than peak4. Finally, peak5 at 2571 cm^{-1} represents the free water group, which has no hydrogen bond [20]. In the ETFE-PEMs, water molecules without hydrogen bonds can only be located in free-volume holes and only have physical interactions (HOH… F) or as surface waters [20, 22]. This water group is not affected by hydrogen bonds, so it has the highest energy and, thus, it is located at the largest wavenumber among the five water components. The above results indicate that even under dried conditions, the membranes contain water molecules in different states. It is interesting that free water (non-H-bonded water) is also trapped in the membranes.

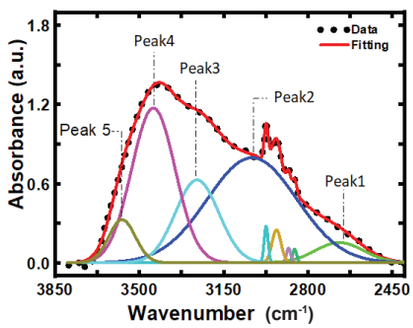

Fig. 4. A deconvolution model for the FT-IR spectrum of ETFE-PEM with GD=10.2% in the spectral region of 2400-3800 cm^{-1}.

Figure 5A shows the spectrum of each component's peak in the band region of 2400-3800 cm^{-1} and the results indicate that the peak positions of all samples are nearly unchanged with GD, which is similar to that in the spectral region of 1500-2000 cm^{-1}. Fig. 5B shows the peak area of each component peak, and the results indicate that the peak areas significantly change with GD and follow the order of peak2 $[(SO_3)…(H_3O^+)(H_2O)_n]$ > peak4 $(H_2O…H_2O)$ > peak3 $(H_5O_2^+)$ > peak1 (H_3O^+) > peak5 (HOH…F). Peak3 $(H_5O_2^+)$ is of the -OH group in the large protonate groups, which can form the Zundel $(H_5O_2^+)$ because as GD increases, the elongated PSSA chains reach local water clusters in the membrane. Simultaneously, the electrostatic binding force pulls water groups around PSSA chains, which leads to the increase of water content. As GD increases from 19.8 to 30.5%, the surrounding water content also increases. At the same time, the -OH bond in the large protonate groups is formed diverse, possibly in Zundel $(H_5O_2^+)$. Therefore, the same -OH group in large protonate groups exhibits multiple components leading to the increase of

peak area with GD [19, 22]. The water state of $((SO_3)\ldots(H_3O^+)(H_2O)_n)$ is the most dominant and located mainly around the PSSA chains, but these water amounts are not large enough to form water channels, which is entirely consistent with those in the spectral region of 2400-3800 cm^{-1}.

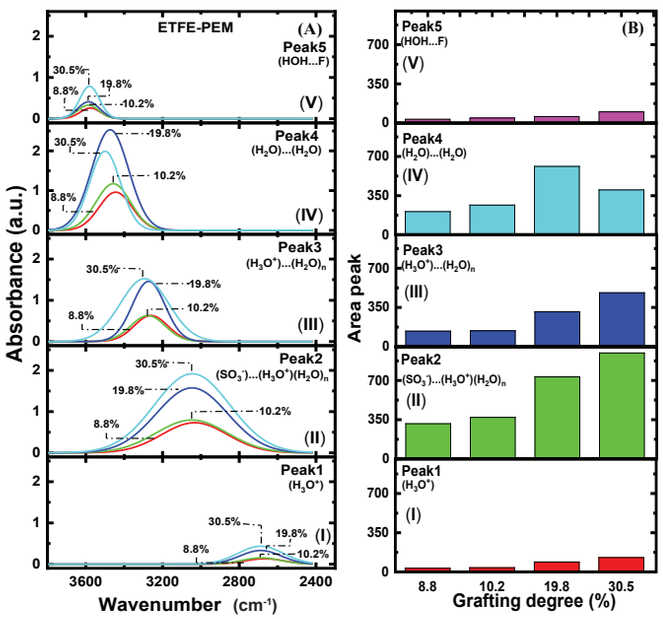

Fig. 5. FT-IR spectra of ETFE-PEMs with GD=8.8-30.5% in the band region of 2400-3800 cm^{-1} for (A) each component peak and (B) the corresponding peak area.

Figure 6 shows the total peak areas of the ETFE-PEMs with GD=8.8-30.5% in the spectral region of (A) 1500-2000 cm^{-1} and (B) 2400-3800 cm^{-1}. Interestingly, the total peak areas in both regions increase quickly and linearly with GD in the range of 8.8-19.8% and then increase more slowly as GD increases to 30.5%. In other words, the increase occurs via two steps even at ambient conditions. The increase of total peak area with GD can be explained by the fact that the membrane with higher GD possesses a higher number of $-SO_3H$ groups, thus possessing more water molecules [7]. The increase via two steps should be related to the hierarchical structure change of ETFE-PEMs, in which the lamellar period and oriented crystallite sizes (i.e., lamellar grain sizes) increased quickly in the GD of 0-19% and then more slowly with higher GD, as observed by small- and ultra-small angle X-ray scattering (SAXS/USAXS) [9]. The increase of the lamellar period and lamellar grain sizes indicate that the PSSA grafts were generated in the amorphous region of lamellar structures and/or in the regions between two lamellar grains. These newly generated graft phases can absorb water molecules as observed by SAXS/USAXS when measuring the ETFE-PEMs under dry and hydrated states [9]. Thus, the result depicted in Fig. 6 provides the first evidence that the higher-order structure change of ETFE-PEMs in the low GD range of 8.8-30.5% relates closely to their water content even at ambient conditions.

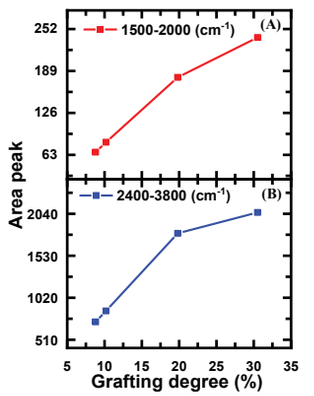

Fig. 6. The total peak area of ETFE-PEMs with GD=8.8-30.5% in the spectral region of (A) 1500-2000 cm^{-1} and (B) 2400-3800 cm^{-1}.

From the basic FT-IR analysis of ETFE-PEMs, the water states inside the membranes are classified into four types [20] including protonated water, water H-bonded to other water molecules, water H-bonded to sulfonic acid groups, and non-H-bonded water as depicted in Fig. 7. Protonated water plays an essential role in proton conductance for fuel cells since, in its hydronium form, protons are transported via a diffusion mechanism that occurs when the water content is low [19]. When the number of water molecules increases at low temperatures, water binds with H_3O^+ to form a hydrogen-bonding network such as Zundel ($H_5O_2^+$), Eigen ($H_9O_4^+$), etc., and thus are separated from the SO_3^- group and tend to diffuse through the membranes [23]. The water group, which directly interacts with the $-SO_3H$ group, results in the dissociation of hydrogen to form SO_3^- and H_3O^+ [19] and then to transport proton through the oscillations of polymer chains due to the attraction between the SO_3^- and H_3O^+ groups. The water form that does not interact with H_3O^+ but interacts through hydrogen bonds is the most important water group because they are sensitive to RH and play an important role in transporting protons across the membrane [24]. The remaining water form is the so-called free water as it may be trapped in the voids (or free-volume holes) without hydrogen or water bonds. This amount of water is not significant and does not contribute to proton conductance, nonetheless, it is difficult to remove even after drying and can also cause membrane swelling.

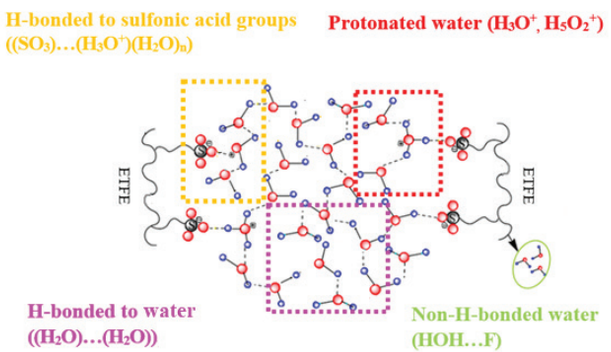

Fig. 7. A proposed model of the water states in ETFE-PEM.

Conclusions

Detailed analysis of the FT-IR spectra of ETFE-PEMs with GD=8.8-30.5% provides an observation of component waters in the two broader bands of 1500-2000 cm^{-1} and 2400-3800 cm^{-1} that include protonated water (H_3O^+, $H_5O_2^+$), H-bonded water to sulfonic acid groups $((SO_3)\ldots(H_3O^+)(H_2O)_n)$, H-bonded water to other water molecules $((H_2O)\ldots(H_2O))$, and non-H-bonded water (HOH…F) at ambient conditions in which the water form of $((SO_3)\ldots(H_3O^+)(H_2O)_n)$ is mainly represented. The free water (non-H-bonded water) is assumed to be in the holes of the ETFE matrix and, hence, this is the most difficult water to remove under conditions of 50°C for 24 h. The total peak areas of the water molecules dramatically increase with the increase of GD indicating that the ETFE-PEM with higher GD possesses higher water content. The increase of these total peak areas with GD via two steps revealed the important relationship between the higher-order structures and the capacity for water content at ambient conditions. Note that these observed contents can have a significant effect on the conductance of ETFE-PEMs under the conditions of low relative humidity and on the results of measurements of certain characterisations or testing methods.

ACKNOWLEDGEMENTS

This work was funded by Vingroup Big Data Institute (VINBIGDATA), Vingroup and supported by Vingroup Innovation Foundation (VINIF) under project code VINIF.2020.DA08.

COMPETING INTERESTS

The authors declare that there is no conflict of interest regarding the publication of this article.

REFERENCES

[1] I. Staffell, et al. (2019), "The role of hydrogen and fuel cells in the global energy system", *Energy & Environmental Science*, **12(2)**, pp.463-491.

[2] G. Frenette, D. Forthoffer (2009), "Economic & commercial viability of hydrogen fuel cell vehicles from an automotive manufacturer perspective", *International Journal of Hydrogen Energy*, **34(9)**, pp.3578-3588.

[3] J. Garche, L. Jürissen (2015), "Applications of fuel cell technology: status and perspectives", *The Electrochemical Society Interface*, **24(2)**, pp.39-43.

[4] J.W. Kulikowska, et al. (2017), "Polymers application in proton exchange membranes for fuel cells (PEMFCs)", *Physical Sciences Reviews*, **2(8)**, pp.293-348.

[5] T. Li, et al. (2020), "Performance comparison of proton exchange membrane fuel cells with Nafion and Aquivion perfluorosulfonic acids with different equivalent weights as the electrode binders", *ACS Omega*, **5**, pp.17628-17636.

[6] L. Gubler, et al. (2009), "Novel ETFE based radiation grafted poly (styrene sulfonic acid-co-methacrylonitrile) proton conducting membranes with increased stability", *Electrochemistry Communications*, **11(5)**, pp.941-944.

[7] T.D. Tap, et al. (2018), "Humidity and temperature effects on mechanical properties and conductivity of graft-type polymer electrolyte membrane", *Radiation Physics and Chemistry*, **151**, pp.186-191.

[8] T.D. Tap, et al. (2013), "Poly(ethylene-co-tetrafluoroethylene) (ETFE)-based graft-type polymer electrolyte membranes with different ion exchange capacities: relative humidity dependence for fuel cell applications", *Journal of Membrane Science*, **447**, pp.19-25.

[9] T.D. Tap, et al. (2014), "Hierarchical structure-property relationships in graft-type fluorinated polymer electrolyte membranes using small- and ultrasmall-angle X-ray scattering analysis", *Macromolecules*, **47(7)**, pp.2373-2383.

[10] J. Chen, et al. (2007), "Polymer electrolyte hybrid membranes prepared by radiation grafting of p-styryltrimethoxysilane into poly (ethylene-co-tetrafluoroethylene) films", *Journal of Membrane Science*, **296(1-2)**, pp.77-82.

[11] J. Chen, et al. (2006), "Preparation and characterization of chemically stable polymer electrolyte membranes by radiation-induced graft copolymerization of four monomers into ETFE films", *Journal of Membrane Science*, **269(1-2)**, pp.194-204.

[12] M.M. Nasef (2014), "Radiation-grafted membranes for polymer electrolyte fuel cells: current trends and future directions", *Chemical Reviews*, **114**, pp.12278-12329.

[13] S. Slade, et al. (2002), "Ionic conductivity of an extruded Nafion 1100 EW series of membranes", *Journal of the Electrochemical Society*, **149(12)**, pp.1556-1564.

[14] M. Maréchal, et al. (2007), "Solvation of sulphonic acid groups in Nafion® membranes from accurate conductivity measurements",

Electrochemistry Communications, **9(5)**, pp.1023-1028.

[15] G. Çelik, et al. (2016), "Towards new proton exchange membrane materials with enhanced performance via RAFT polymerization", *Polymer Chemistry*, **7(3)**, pp.701-714.

[16] T. Hamada, et al. (2015), "Poly(ether ether ketone) (PEEK)-based graft-type polymer electrolyte membranes having high crystallinity for high conducting and mechanical properties under various humidified conditions", *Journal of Materials Chemistry A*, **3(42)**, pp.20983-20991.

[17] M. Laporta, et al. (1999), "Perfluorosulfonated membrane (Nafion): FT-IR study of the state of water with increasing humidity", *Physical Chemistry Chemical Physics*, **1(19)**, pp.4619-4628.

[18] M. Chaplin (2009), "Theory vs experiment: what is the surface charge of water", *Water*, **1**, pp.1-28.

[19] M. Eikerling, et al. (2001), "Mechanisms of proton conductance in polymer electrolyte membranes", *The Journal of Physical Chemistry B*, **105(17)**, pp.3646-3662.

[20] D.W. Hofmann, et al. (2009), "Investigation of water structure in Nafion membranes by infrared spectroscopy and molecular dynamics simulation", *The Journal of Physical Chemistry B*, **113(3)**, pp.632-639.

[21] J. Kim, et al. (2002), "The vibrational spectrum of the hydrated proton: comparison of experiment, simulation, and normal mode analysis", *The Journal of Chemical Physics*, **116(2)**, pp.737-746.

[22] H. Nishiyama, et al. (2020), "Chemical states of water molecules distributed inside a proton exchange membrane of a running fuel cell studied by operando coherent anti-stokes Raman scattering spectroscopy", *The Journal of Physical Chemistry C*, **124(18)**, pp.9703-9711.

[23] H. Gao, K. Lian (2014), "Proton-conducting polymer electrolytes and their applications in solid supercapacitors: a review", *RSC Advances*, **4(62)**, pp.33091-33113.

[24] K.D. Kreuer, et al. (2004), "Transport in proton conductors for fuel-cell applications: simulations, elementary reactions, and phenomenology", *Chemical Reviews*, **104(10)**, pp.4637-4678.